Supplementary Material (ESI) for Dalton Transactions

Supplementary materials

Ferromagnetic Coupling in Oximato-Bridged Multi-Decker Ni^{II} Clusters

Hui-Zhong Kou,*[a] Guang-Yu An,[a] Cong-Min Ji,[a] Bing-Wu Wang,*[b] Ai-Li Cui[a]

[a] Department of Chemistry, Tsinghua University, Beijing 100084, P. R. China. Fax: (+86)-10-62771748
E-mail: kouhz@mail.tsinghua.edu.cn

[b] State Key Laboratory of Rare Earth Materials Chemistry and Applications, College of Chemistry and Molecular Engineering, Peking University, Beijing 100871 (P. R. China). E-mail: bwwang@pku.edu.cn

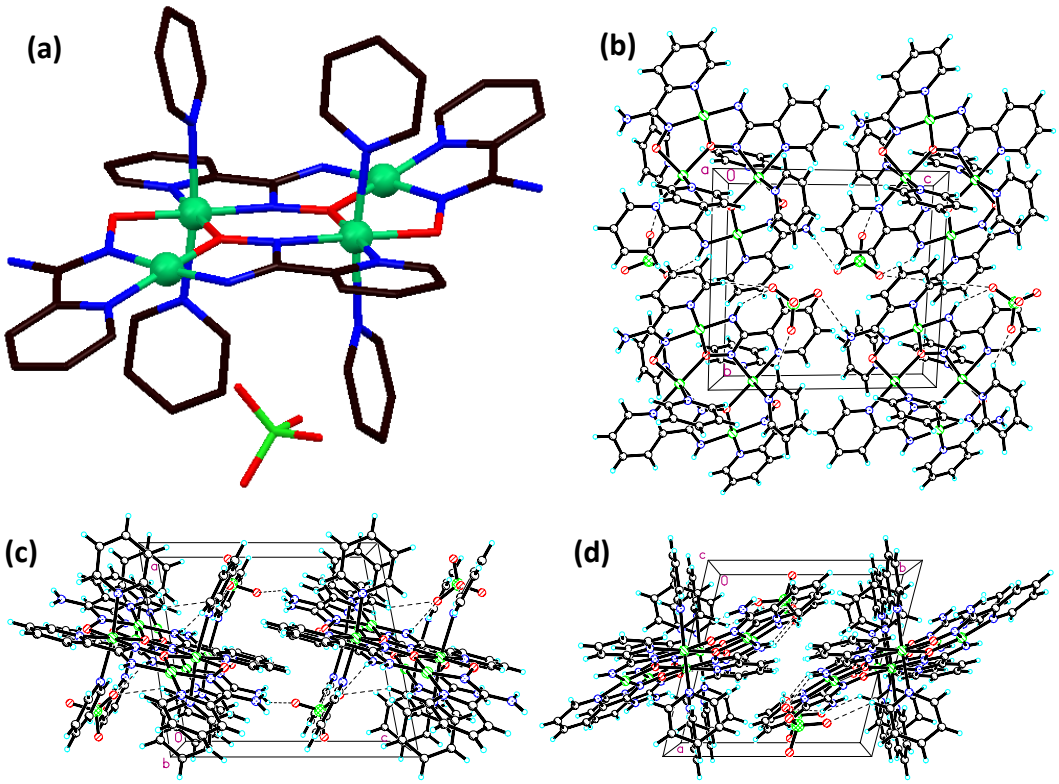

Fig. S1. (a) Top view of the molecular structure of the single-decker Ni_4 compound **1**. (b-d) Cell packing diagrams along the *a*, *b* and *c* axis, respectively, showing the intermolecular hydrogen bonding interactions.

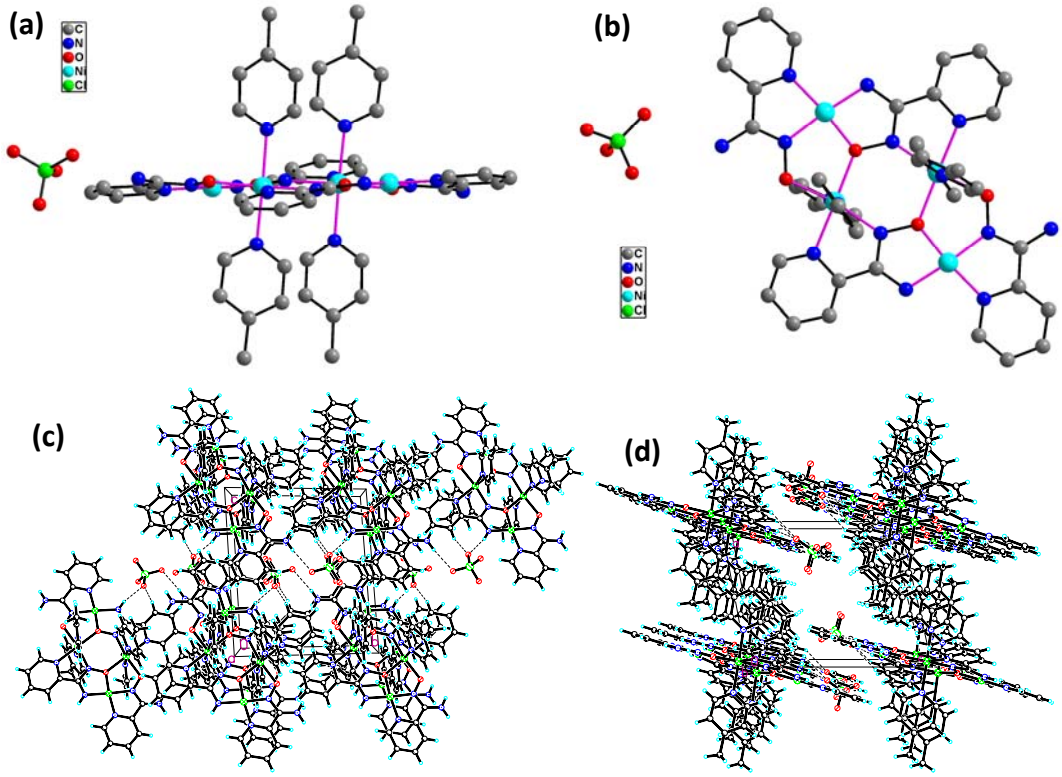

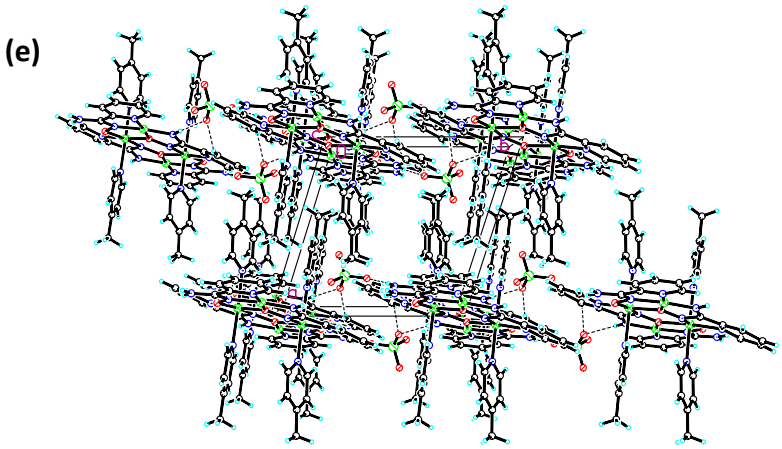

Fig. S2. (a and b) Side and top views of the molecular structure of the single-decker Ni_4 compound **2**. (c-e) Cell packing diagrams along the *a*, *b* and *c* axis, respectively, showing the intermolecular hydrogen bonding interactions.

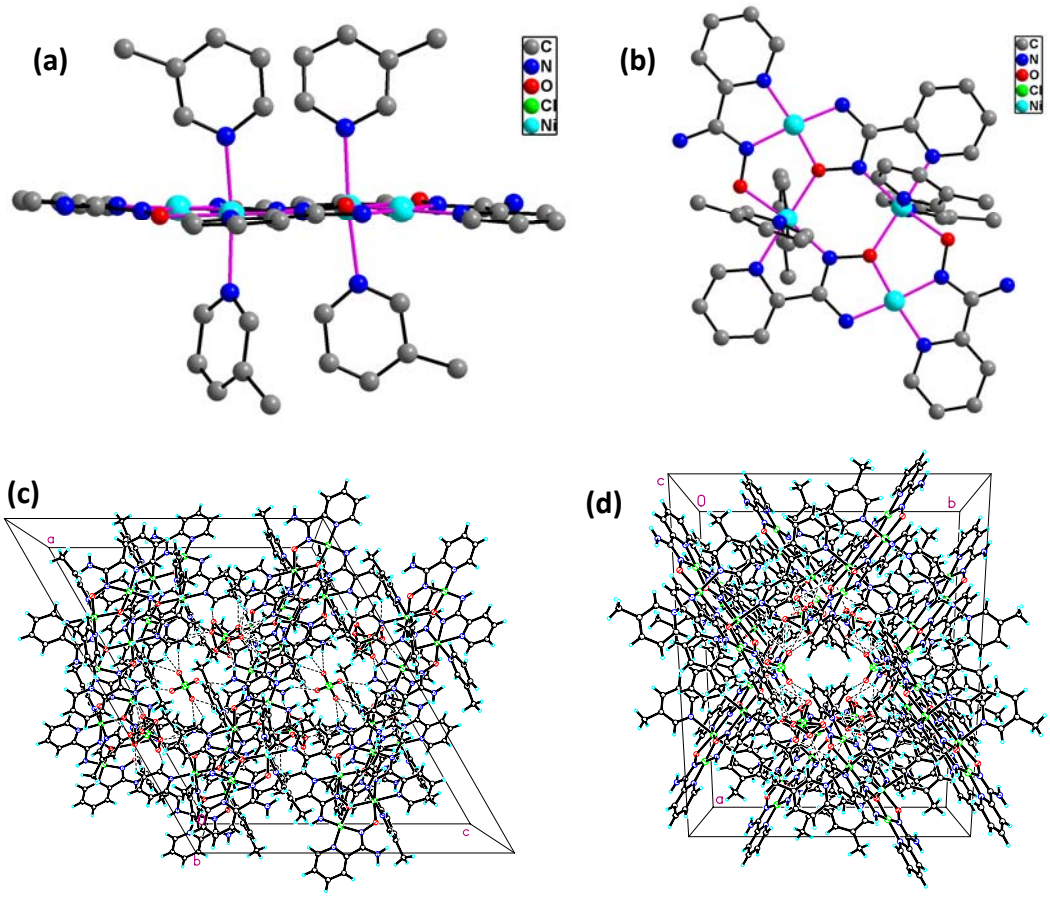

Fig. S3. (a and b) Side and top views of the molecular structure of the single-decker $[Ni_4]^{2+}$ cation in compound **3**. (c and d) Cell packing diagrams along the *b* and *c* axis, respectively, showing the intermolecular hydrogen bonding interactions.

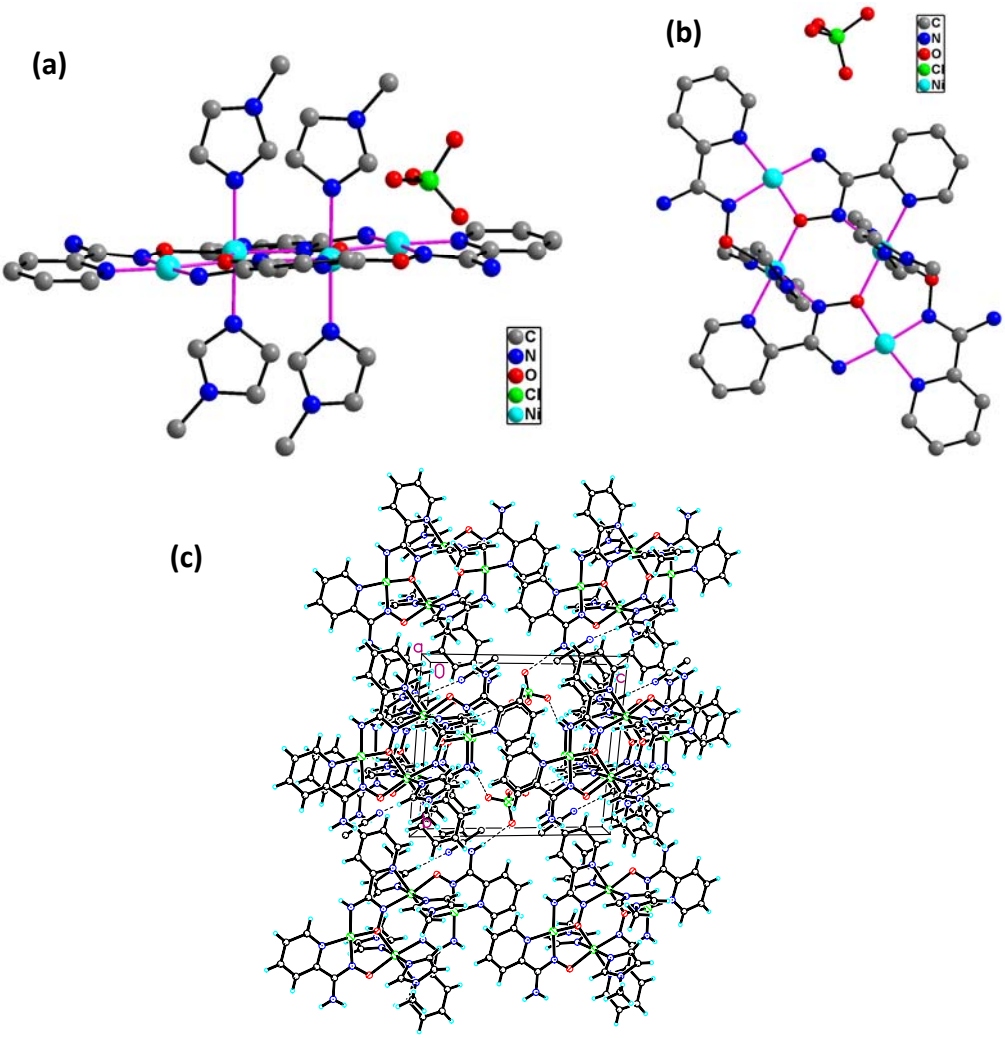

Fig. S4. (a and b) Side and top views of the molecular structure of the single-decker $[Ni_4]^{2+}$ cation in compound **4**. (c) Cell packing diagram along the *a* axis, showing the intermolecular hydrogen bonding interactions.

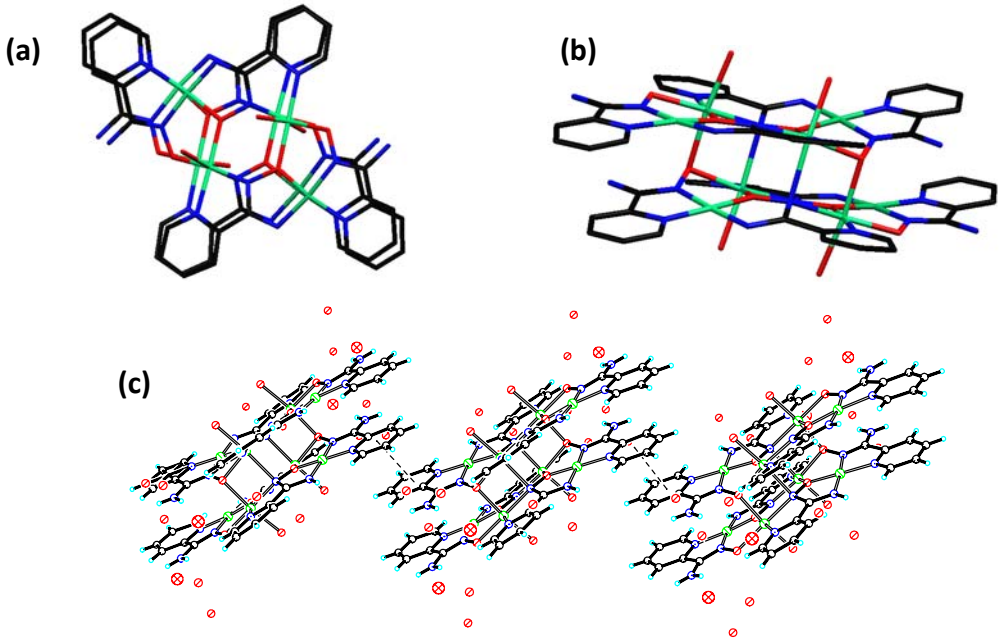

Fig. S5. (a and b) Top view of the molecular structure of the double-decker Ni_8 compound **5**. (c) Intermolecular π---π interaction in compound **5**.

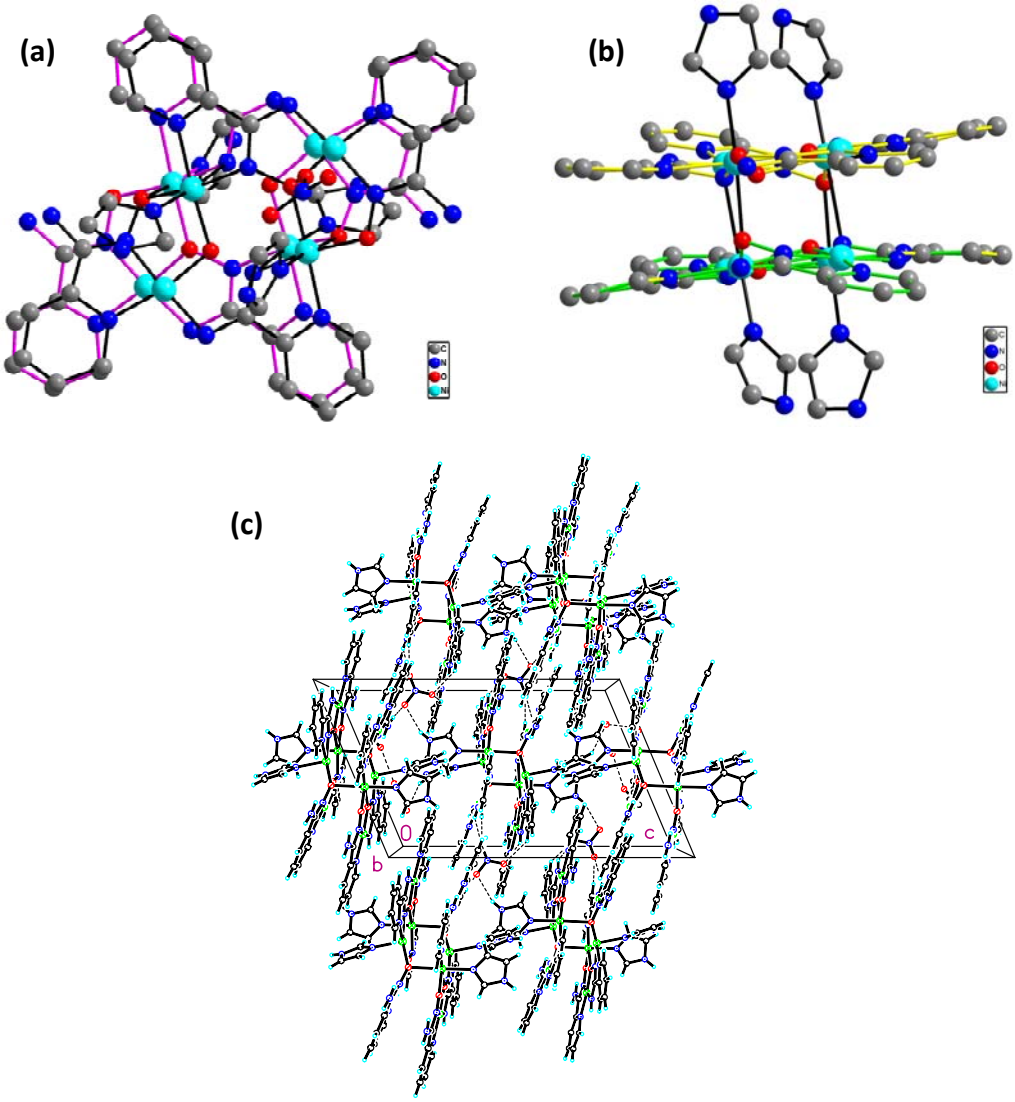

Fig. S6. (a and b) Top and side views of the molecular structure of the double-decker Ni_8 compound **6**. (c) Cell packing diagram along the *b* axis, showing the intermolecular hydrogen bonding interactions.

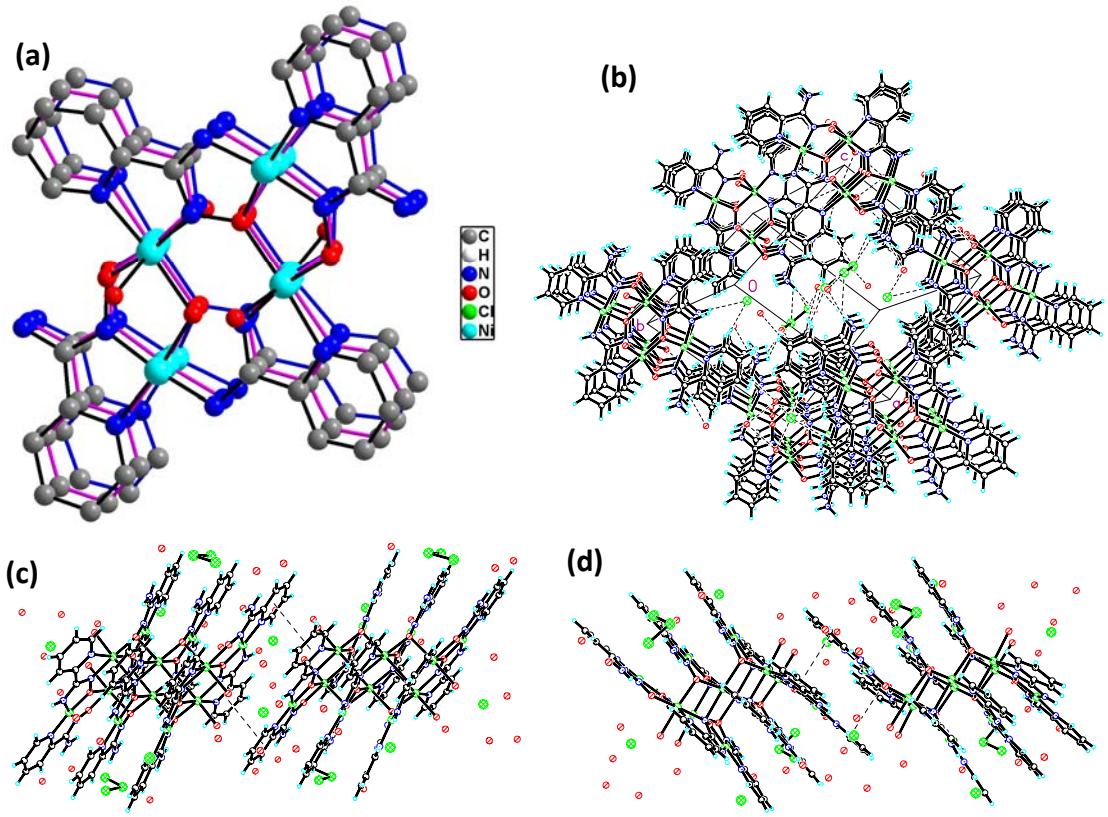

Fig. S7. (a) Top view of the molecular structure of the triple-decker Ni_{12} compound **7**. (b) Cell packing diagram showing the intermolecular hydrogen bonding. (c) Intermolecular π---π interaction in compound **7**.

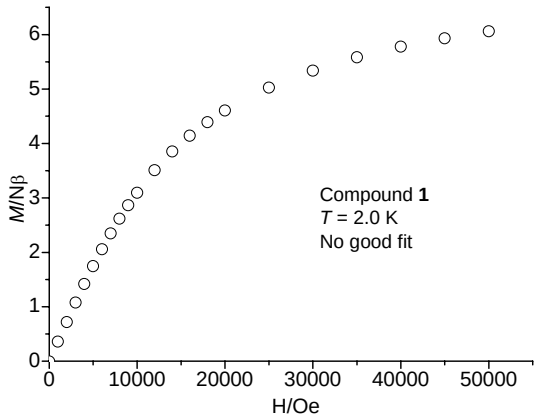

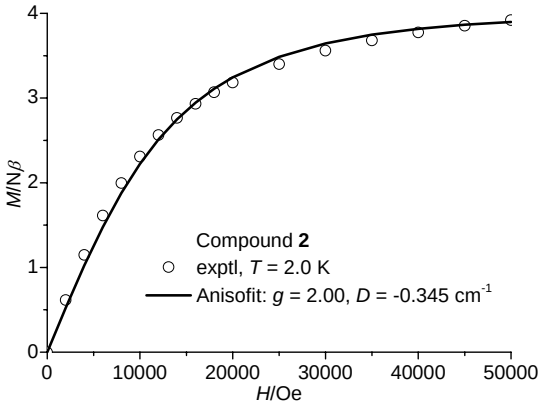

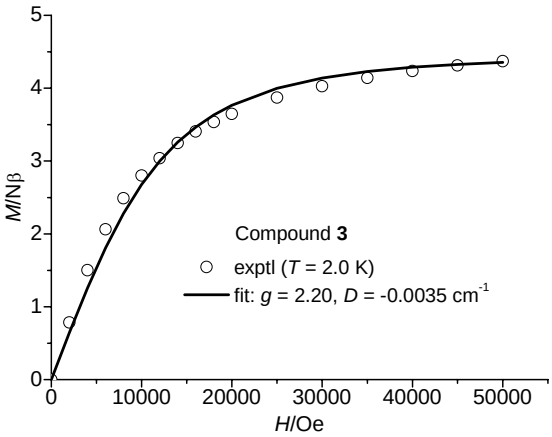

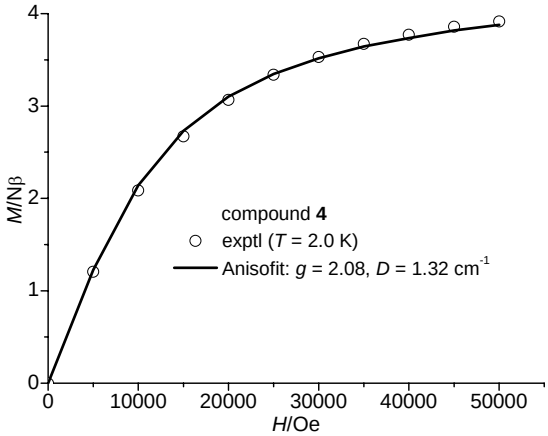

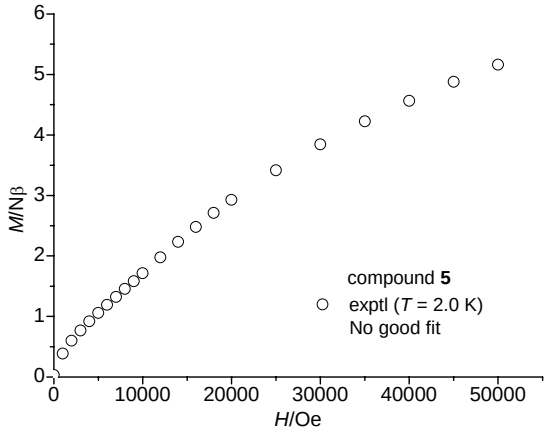

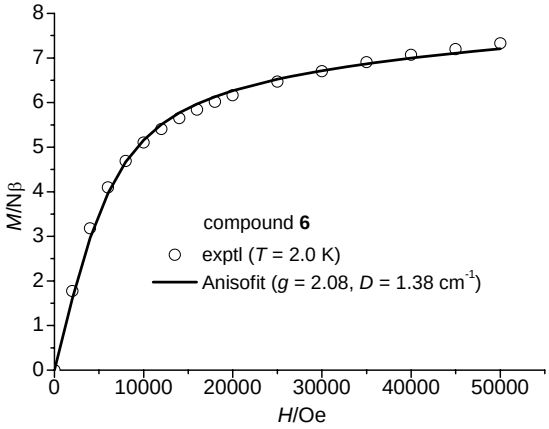

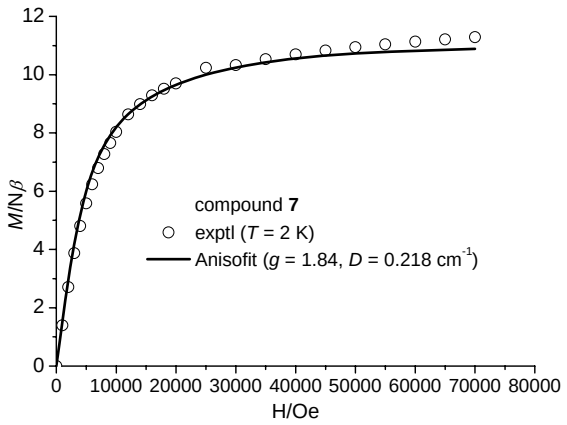

Fig. S8. The field-dependence of complexes **1**-**7**. The solid lines are the fit results for S = 2 (compounds **1**-**4**), 4 (compounds **5** and **6**), 6 (compound **7**) using the parameters shown in the plots.

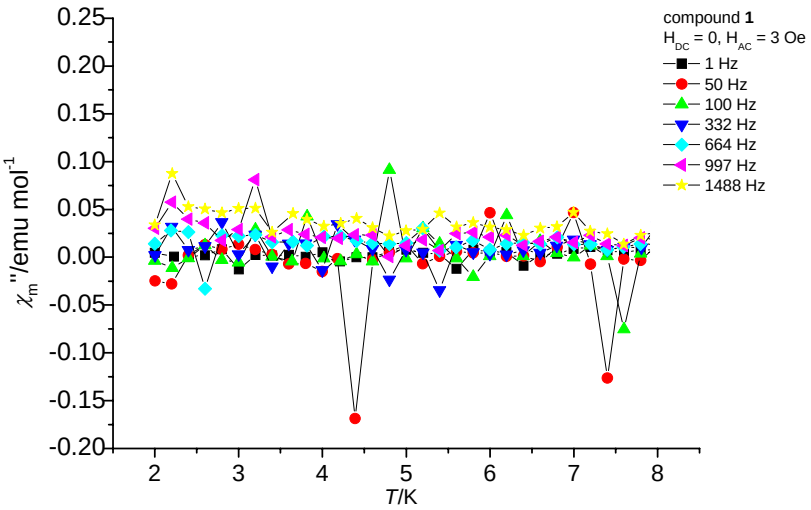

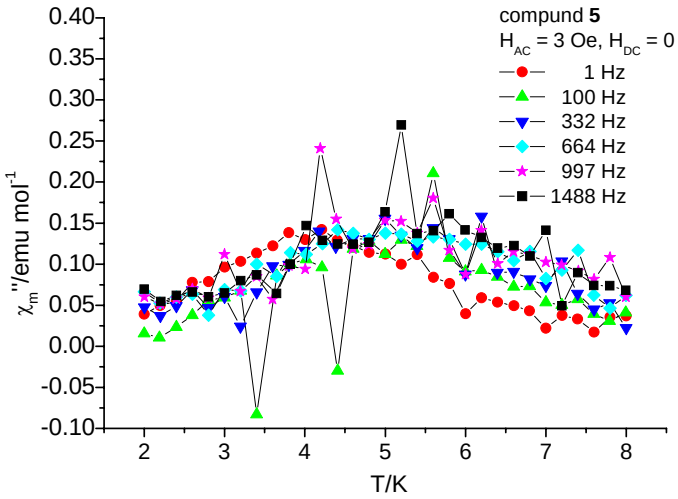

Fig. S9. Out-of-phase AC magnetic susceptibilities of complexes **1** and **5** measured under zero DC magnetic field.

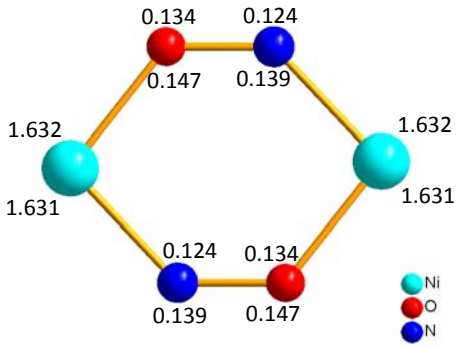

Fig. S10. Spin population distribution of the model dinuclear $Ni(NO)_2Ni$ system. The upper values nearby the atoms are corresponding spin population for the model with N-O bond distance 1.42 Å, and the lower for 1.35 Å.

N-O: 1.42 Å

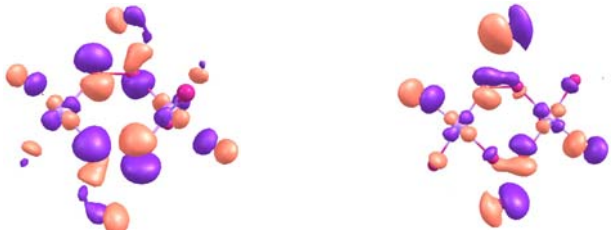

SOMO1 e_1= 0.07368 au, SOMO2 e_2= 0.04683 au

N-O: 1.35 Å

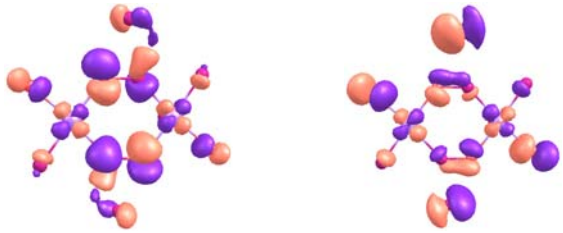

SOMO1' e_1'= 0.07442 au, SOMO2' e_2'= 0.04139 au

Fig. S11. Singly occupied molecular orbitals (SOMO) and corresponding orbital energies for the model $Ni(NO)_2Ni$ system. SOMO1, SOMO2 are the results of N-O bridge 1.42 Å and SOMO1', SOMO2' for N-O bridge 1.35 Å, respectively.